

Selectivity and Safety of VIP943: A Novel CD123 Targeting Antibody-Drug Conjugate (ADC) Using a Proprietary Linker and Payload Class

Poster # 1435

Beatrix Stelte-Ludwig, PhD¹, Tibor Schomber, PhD¹, Raquel Izumi, PhD², Harvey Wong, PhD², Melanie M. Frigault PhD², Anne-Sophie Rebstock, PhD¹, Sebastian Ludwig, PhD¹, Arushi Mithal², Amy J. Johnson, PhD² and Ahmed Hamdy, MD²

¹Vincerox Pharma GmbH, Monheim, Germany, ²Vincerox Pharma, Inc., Palo Alto, CA, USA

INTRODUCTION

ADCs as therapeutic class have been highly efficacious but suffer from shortcomings in their safety profile. Most payloads are cytotoxic agents that can inhibit general processes of cellular homeostasis including microtubule polymerization or DNA damage repair. While these are good targets for cytotoxicity, they have the drawback of being non-selective for dividing cancer cells. Here, we report the potent on-target activity and high selectivity of our new CD123-targeting ADC VIP943, which utilizes a kinesin spindle protein inhibitor (VIP176), modified with a CellTrapper[®] moiety to avoid membrane permeability¹. The kinesin super family is comprised of motor-proteins involved in various cellular mechanisms. The target of our payload is the kinesin spindle protein (KSP) also known as KIF11 or Eg5. KSP is a motor protein essential for the formation of the bipolar mitotic spindle during cell division in the G2/M phase. Targeting this motor protein enables us to specifically inhibit dividing cells, while at the same time avoiding off-target toxicities in non-dividing differentiated cells.

METHODS

Eg5 on-target and KIF family selectivity biochemical assay. The motor domain of the human Eg5 (KSP, 10 nM) and of other KIF family members were evaluated in a biochemical assay using stabilized microtubules (50 µg/ml). The freshly prepared mixture was incubated with VIP176 (payload of VIP943 starting at 10 µM (1:10 dilution), S-Trityl-L-Cysteine (STLC, a reversible first generation KSP, and ipinesib, a clinical stage KSP (starting concentration 10 µM) in the presence of 500 µM ATP. ATPase activity was directly analyzed by measuring formed inorganic phosphate by determination of complex formation with Malachite green after 50 min at 1620 nm.

Cell cycle analysis. The effect of VIP943 on the 3 phases of the cell cycle (G0/G1- S- G2/M) was measured with DNA staining (200 µL propidium iodide (Merck/Sigma, #P4170, 100 µg/ml in PBS, 4°C) and flow cytometry in MOLM-13 and MV-4-11 cell lines (2x10⁶ cells/well). Concentrations of VIP943 of 5 to 500 nM were used for a 48 h treatment of cells. Then DNA staining of the treated and untreated cells was evaluated by flow cytometry (MacsQuant, Millipore, Germany). In addition, cell cycle analysis was measured by flow cytometry after a 4 h incubation with VIP943 (20 nM) in MOLM-13 cells. The corresponding isotype ADC was used as a control. After a final incubation time of 48 h, 72 h and 96 h, the analysis was performed. Flow cytometry was designed to ensure only single cell evaluation.

In vitro cytotoxicity. A cell line panel containing 56 hematologic cell lines was treated in vitro with VIP331 (cell permeable analog of VIP176) starting from a top concentration of 12 µM with 3.16-fold serial dilutions to achieve 9 dose levels where the lowest VIP331 concentration was 120 pM. In this study, the 50% inhibitory concentration (IC₅₀) was determined in cancer cell lines using CellTiter-Glo luminescent cell viability assay. Each cell line was treated with test article VIP331 and culture medium containing 0.25% (v/v) DMSO as vehicle control. Cell viability was determined after a 72-hour incubation. Clinically impactful biomarkers for agents used for the treatment of hematologic malignancies were extracted and mapped from CCL-...¹⁻⁴

Receptor occupancy. MOLM-13 cells or human whole blood were incubated with different concentrations of the cold unlabeled 7G3 antibody in duplicate. To reduce unspecific binding, an FC block was carried out in advance. After the first staining, PE-Alexa antibody mixture is added to each bucket, incubated, washed and measured with FACS Canto II (BD).

Nonhuman primate safety and toxicokinetics. VIP943 was intravenously (IV) administered to Cynomolgus monkeys at 1, 3, or 9 mg/kg once weekly for 4 weeks in a Good Laboratory Practice (GLP) toxicology study. Plasma samples were collected at predose, 0.5, 1, 2, 4, 8, 24, 72, and 168 h post-dose (n=5/group/sex) on study Day 1 and Day 22. Plasma concentrations of total antibody from VIP943 and VIP176 were determined by LC/MS/MS. Toxicokinetics for individual animals was determined using non-compartmental analysis.

RESULTS

On-target activity of VIP176, the non-permeable metabolite of VIP943, was demonstrated in comparison to the permeable KSP inhibitor VIP331 on recombinant motor protein Eg5. The described modification of VIP176 did not influence the inhibitory potency as compared to parental compound VIP331.

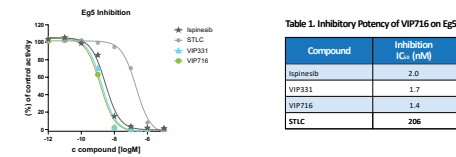


Figure 1. Inhibition of Motor Protein KSP (Eg5): (A) Dose response curves of payload VIP176 (non-permeable) and VIP331 (permeable) vs ipinesib and STLC. (B) Time-dependent distribution of MV-4-11 cells in different cell cycle phases of untreated versus VIP943 (500 nM) treated samples. (C) Time-dependent increase of apoptotic MOLM-13 cells after a 4 hr 20 nM VIP943 pulse treatment followed by an incubation up to 96 h in comparison to the corresponding isotype control ADC (VIP156).

Selectivity of VIP943 payload on different KIF family members

The impact of VIP176 (VIP943 payload with CellTrapper) was evaluated on different KIF family members compared to ipinesib and the permeable payload VIP331 at concentrations up to 10 µM. VIP176, VIP331, and ipinesib are highly selective for KSP (Eg5) and showed no activity against other KIF family members (Table 2).

Table 2. Selectivity of VIP176 to 11 KIF family members.

KIF Family Member	Biological Function	VIP176 (IC ₅₀)	VIP331 (IC ₅₀)	ipinesib (IC ₅₀)
Eg5/KSP	kinesin spindle assembly and alignment of chromosome	1.4	1.7	2.0
KIF18	transport of mitochondria and synaptic vesicle towards neurite	no inhibition (10 µM)	no inhibition (10 µM)	no inhibition (10 µM)
KIF2	transports membranous organelles	no inhibition (10 µM)	no inhibition (10 µM)	no inhibition (10 µM)
KIF3C	axon growth, regeneration by regulating microtubule cytoskeleton in the growth cone	no inhibition (10 µM)	no inhibition (10 µM)	low inhibition at 10 µM
KIF13B	reorganization of the cortical cytoskeleton; regulates axon formation	no inhibition (10 µM)	no inhibition (10 µM)	no inhibition (10 µM)
KIF26A	repressing cell growth in the enteric nervous system	no inhibition (10 µM)	no inhibition (10 µM)	no inhibition (10 µM)
CENP-E / KIF10	metaphase chromosome alignment	no inhibition (10 µM)	no inhibition (10 µM)	no inhibition (10 µM)
MKLP	spindle pole separation	n.d.	no inhibition (10 µM)	no inhibition (10 µM)
KIF1C	cytoskeletal organizing and loop for microtubule transport towards neurite	no inhibition (10 µM)	no inhibition (10 µM)	no inhibition (10 µM)
KIF13C	translocate cargos along microtubules	no inhibition (10 µM)	no inhibition (10 µM)	no inhibition (10 µM)
MACK1/KIF2c	destabilize microtubules; catastrophe frequency increase	no inhibition (10 µM)	no inhibition (10 µM)	no inhibition (10 µM)
KIFC / KIF5	vesicle transport	no inhibition (10 µM)	no inhibition (10 µM)	no inhibition (10 µM)

n.d.: Not Determined

Cell cycle analysis of AML cell lines MV-4-11 and MOLM-13 after VIP943 treatment shifts cells into the G2/M phase

The cell cycle consists of 3 phases: the G0/G1 phase, the S phase and the G2/M phase. In healthy cells, the distribution of cells between the respective phases is stable. Treatment of MV-4-11 cells with VIP943 causes a significant and dose-dependent increase of cells in the G2/M phase which is consistent with inhibition of KSP by VIP176 the payload of VIP943 (A). VIP943 treatment demonstrates a time-dependent shift of MV-4-11 cells from the G0/G1 to the G2/M phase. The number of cells in S-phase remains stable (B). In a 4-hour pulse experiment with VIP943, the number of MOLM-13 cells entering apoptosis increased over an incubation period up to 96h. Treatment of VIP943 but not isotype control (VIP156) causes the increase of apoptotic cells (C).

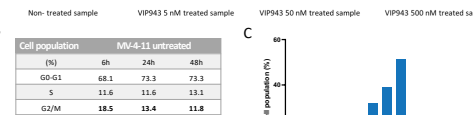
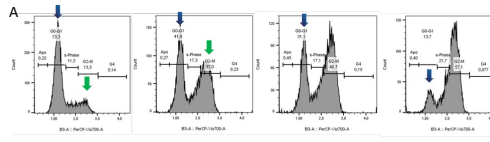


Figure 2. Impact of VIP943 on Cell Cycle: (A) Histograms of MV-4-11 cells treated with VIP943 demonstrating dose-dependent G2/M arrest of cells. Overview of changes in subpopulations after treatment with VIP943 for 48 h. (B) Time-dependent distribution of MV-4-11 cells in different cell cycle phases of untreated versus VIP943 (500 nM) treated samples. (C) Time-dependent increase of apoptotic MOLM-13 cells after a 4 hr 20 nM VIP943 pulse treatment followed by an incubation up to 96 h in comparison to the corresponding isotype control ADC (VIP156).

Sensitivity of VIP943 cell permeable payload VIP331 is not impacted by genomic alterations in a hematologic cell line panel

The impact of genomic biomarkers on in vitro sensitivity of VIP331 in a panel of 56 hematologic cell lines was evaluated. Cell lines are ranked from the lowest to highest IC50 with a mean IC50 of 2.495 nM (range 0.51-30 nM) indicating that most hematologic cell lines tested are sensitive to VIP331. The presence of DNA alterations: AMP (red), HOMDEL (blue), SNV (white/alteration noted) or RNA expression: HIGH (pink), LOW (light blue) in 16 genes associated with hematologic targets including CD123 (IL3RA) do not impact VIP331 cytotoxicity as shown in the heatmap.

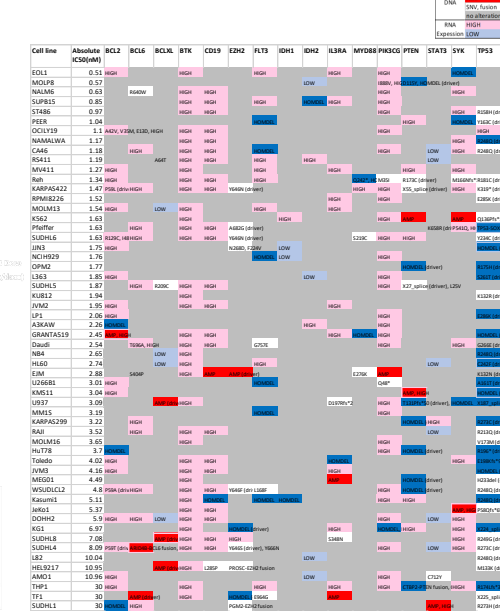


Figure 4. Heat Map of Genomic Biomarkers with In Vitro Cytotoxicity of VIP331. AMP: amplification; HOMDEL: deletion; SNV: single nucleotide variant; HIGH: high mRNA expression; LOW: low mRNA expression

Receptor occupancy competition for binding to CD123 in MOLM-13 AML cell line and in whole blood from healthy human volunteers

PE-labeled 7G3 Ab clone saturates CD123 in MOLM-13 cells and in whole blood in a competition assay.

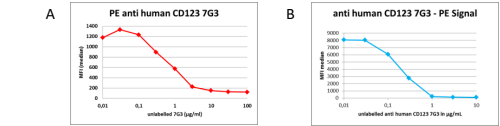


Figure 5. CD123 Receptor Occupancy Assay. (A) MOLM-13 cells (B) whole blood, gated on CD123 positive cells

Nonhuman primate safety and toxicokinetics profile of VIP943 and payload

VIP943 up to 9 mg/kg repeated doses (5 males/5 females per group; QWx4) administered IV were well-tolerated (no mortalities) without adverse events typically observed with ADCs containing other payload classes such as thrombocytopenia, neutropenia, or anemia. Mild signs of fully reversible liver enzyme increases were observed (no morphologic changes). At the highest dose level, ocular findings (corneal pigmentation, single cell necrosis and hypertrophy of the basal cell layer epithelium) were observed at the terminal and recovery ophthalmologic examinations and microscopically at the terminal and recovery neurology intervals. No cardiovascular effects were observed with VIP943 treatment. VIP943 and VIP176 exposures increased with increasing dose in a dose-proportional or greater than dose-proportional manner. No consistent differences in toxicokinetics were observed with sex (combined male and female data is presented). Based on area under the concentration curve (AUC), no accumulation of VIP943 was observed. As well, little to no accumulation was observed for VIP176. Payload to parent ratios (±3%) were consistent with a low level of non-specific release of VIP176 from VIP943.

Table 3. Plasma toxicokinetic parameters (mean ± SD) of total antibody from VIP943* on Days 1 and 22 after weekly IV bolus administration of 1, 3, and 9 mg/kg VIP943 to Cynomolgus monkeys (n=5/sex/dose group)

VIP943 Dose (mg/kg)	Day	C _{max} ** (ng/ml)	AUC _{0-168h} ** (ng·h/ml)	VIP943 Dose (mg/kg)	Day	VIP176-T _{max} ** (h)	VIP176-C _{max} ** (ng/ml)	VIP176-AUC _{0-168h} ** (ng·h/ml)
1	1	0.500(0.500-0.500)	28.9(3.29)	3	1	2.00(2.00-2.00)	183(46.9)	7676(2710)
1	22	0.500(0.500-0.500)	17.5(3.05)	3	22	2.00(2.00-4.00)	649(184)	7123(3550)
3	1	1.000(0.500-4.00)	110(37.3)	3	1	2.00(2.00-4.00)	420(133)	1800(3710)
3	22	0.500(0.500-2.00)	73.5(26.7)	3	22	4.00(2.00-8.00)	943(172)	2000(11300)
9	1	0.500(0.500-2.00)	235(46.7)	9	1	8.00(2.00-8.00)	526(156)	15300(4890)
9	22	0.500(0.500-2.00)	223(49.9)	9	22	4.00(1.61-4.00)	2670(350)	8860(3700)

AUC_{0-168h}** = Area under the concentration-time profile from time 0 to 168 hours post-dose; C_{max}** = Maximum observed plasma concentration; T_{max}** = Time of maximum plasma concentration. *Plasma concentrations of total antibody from VIP943 serve as surrogate for VIP943 concentrations as VIP943 appears to be very stable. ** Median (minimum-maximum)

CONCLUSIONS

On-target selectivity of VIP943 for KSP (Eg5) versus several other KIF family members was confirmed. The on-target activity translates to G2/M arrest in a dose- and time-dependent manner, resulting in apoptosis in AML cell lines. VIP943 permeable payload VIP331 sensitivity in a 56 hematologic cell line panel is independent of common AML genomic alterations such as TP53. Receptor occupancy can be measured using 7G3 Ab clone against CD123 in cell lines and in human whole blood. Based on high selectivity of the targeting Ab and low payload (VIP176) release in the plasma, repeat dosing of VIP943 was well tolerated in Cynomolgus monkeys.

VIP943 is being evaluated in a Phase 1 dose-escalation study in patients with CD123+ hematologic malignancies (NCT06034275). VIP943 completed the first dose cohort (n=3) and is now enrolling in the second dose cohort; consistent with preclinical findings, no safety signals have been observed.

REFERENCES

1. Kirchoff et al. Cancer. 2020
2. cBio portal access 20 March 2023.
3. Gao et al. Science Signaling. 2013
4. Cerami et al. Cancer Discovery. 2012

ACKNOWLEDGMENTS

Special thanks to Gerhard Semstner (Navis ICB, Berlin, Germany) for performing in vitro studies and Henryk Bubik for biochemical assay support. Also special thanks to Charles River Laboratories for performing the safety study.